

Bismuth-containing layered double hydroxide as a novel efficient photocatalyst for degradation of methylene blue under visible light

Mohammad Dinari¹ · Mohamad Mohsen Momeni¹ · Zahra Bozorgmehr¹ · Shiva Karimi¹

Received: 27 April 2016 / Accepted: 24 November 2016 / Published online: 28 November 2016
© Iranian Chemical Society 2016

Abstract Layered double hydroxide (LDH)-based photocatalysts have emerged as a very promising candidate to replace TiO₂, owing to their unique layered structure, tunable band gaps, low cost, ease of scale-up, and good photocatalytic activity. Bismuth-doped ZnCr-LDH was studied as photocatalyst in the photodegradation of methylene blue (MB). The structure and morphology of ZnCr-LDH and ZnCrBi-LDH were characterized using a different mode of delegated tools, e.g., FTIR, XRD, UV–Vis, FESEM–EDX, and TEM measurements. FESEM and TEM image of the synthesized LDHs showed that the synthesized LDH is smooth overlapping crystals, and they are approximately in hexagonal form. The material was found to be a good photocatalyst for degradation of methylene blue in visible light, and the results showed that the photocatalytic activity of ZnCrBi-LDH sample is higher than of ZnCr-LDH sample. According to the kinetic data, the reaction rate constant of ZnCrBi-LDH is approximately four times higher than the apparent reaction rate constant of ZnCr-LDH. The catalytic activity was retained even after four methylene blue degradation cycles, indicating that the LDH could be an important addition to the field of wastewater treatment.

Keywords Photocatalytic activity · Visible light · Layered double hydroxide (LDH) · Methylene blue

Introduction

Our surrounding environment continues to become more polluted, and the conventional chemical methods that contract with environmental pollution have been unable to meet the requirements of modern energy-saving themes and environmental protection [1]. Environmental problems induced by toxic and hardly degradable organic pollutants have posed a grave menace to human well-being and development in the twenty-first century. Semiconductor photocatalysis has attracted increasing interest and been recognized as a “green” and efficient strategy in the field of environmental remediation because it can directly utilize sunlight as the energy source [2]. In the development of efficient photocatalytic systems, the synthesis of high-performance photocatalysts performed under visible light remains most important [3].

In particular, the rapid growth in nanotechnology and nanomaterial synthesis has created a large amount of promising photosensitive semiconductor materials [3–5]. Of the common photosensitive semiconductors, TiO₂ has proved to be the most promising photocatalyst in the degradation of dyes and pollutants in wastewater streams and contaminated air [6, 7]. This is attributed to its wide band gap (3.2 eV) and the frequent recombination of the photogenerated electron–hole pairs. The large band gap of 3.2 eV restricts the activation of TiO₂ to high-energy UV radiation. Unfortunately UV radiation accounts for less than 5% of solar light and less than 0.1% of indoor lighting. To better utilize visible light that accounts for 43% of solar energy, efforts have been made to exploit visible light-responsive photocatalysts [6, 8].

Visible light-driven photocatalysis is highly expected to be an ideal “green” technology for remediation of

✉ Mohammad Dinari
dinari@cc.iut.ac.ir; mdinary@gmail.com

✉ Mohamad Mohsen Momeni
mm.momeni@cc.iut.ac.ir

¹ Department of Chemistry, Isfahan University of Technology, Isfahan 84156-83111, Islamic Republic of Iran

environment pollution, hydrogen energy production from water and CO₂ fixation, etc. [9–11].

Developing new materials has become a hot topic in order to improve the efficiency of degradation of dye and other molecules using just sunlight [12]. In the recent years, a lot of attention has been focused on preparing the adsorption material with low-cost and high adsorption capacity, like clay minerals, polymers, nanomaterials, and silica [12–16].

Among the alternative semiconductor photocatalysts that have been explored to date, layered double hydroxide (LDH)-based photocatalysts have emerged as a very promising candidate to replace TiO₂, owing to their unique layered structure, tunable band gaps, low cost, ease of scale-up, and good photocatalytic activity for water splitting and other reactions [17–23]. LDHs are a family of 2D layered anionic clays with the general formula $[M_{1-x}^{2+}M_x^{3+}(\text{OH})_2] [(A^{n-})_{x/n} \cdot m\text{H}_2\text{O}]$, where M²⁺ is a divalent metal ions such as Mg²⁺, Fe²⁺, Cu²⁺, Co²⁺, and Ca²⁺, M³⁺ is a trivalent metal ions such as Al³⁺, Cr³⁺, Fe³⁺, Co³⁺, Mn³⁺, and Ga³⁺, and Aⁿ⁻ is an interlayer anion, such as Cl⁻, CO₃²⁻, F⁻, NO₃⁻, polyoxometalate and various organic anions and *x* is the M³⁺/(M²⁺ + M³⁺) molar ratio that the pure phase of LDHs is usually obtained for a restricted range as 0.2 ≤ *x* ≤ 0.33 [24–28]. The anions and divalent cations in these materials are often easily exchanged, which allows great flexibility in the composition and electronic structure of LDHs. By incorporating particular photoactive metal cations into LDHs, visible light-responsive photocatalysts with band gaps from 2.0 to 3.4 eV can be synthesized. Furthermore, by controlling the particle size, surface defects can be introduced that alter the LDH electronic structure and greatly enhance the efficiency of photogenerated charge separation and photocatalytic reactions rates. LDHs thus offer a robust structural platform for the development of novel semiconductor photocatalysts with high visible light activity, motivating detailed experimental and theoretical investigations in this area [29, 30].

Here we developed a ZnCrBi-LDH hybrid to improve the photocatalytic properties of ZnCr-LDH which may be applied in wastewater treatment. The composites were characterized by X-ray diffraction (XRD), Fourier transfer infrared (FTIR), field emission scanning electron microscopy (FESEM), and transmission electron microscopy (TEM) techniques and other features to reveal the material's morphology and other features. The photocatalytic degradation experiments of methylene blue (MB) dyes with ZnCrBi-LDH composite were conducted to show that a higher visible light-driven degradation of organic pollutants could be obtained. ZnCrBi-LDH composite photocatalyst exhibited much high photocatalytic activity as compared to ZnCr-LDH alone.

Experimental

Materials

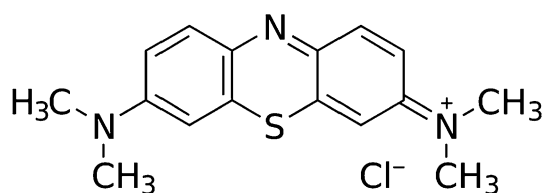
Zinc nitrate hexahydrate [Zn(NO₃)₂·6H₂O], chromium nitrate nonahydrate [Cr(NO₃)₃·9H₂O], and bismuth(III) nitrate pentahydrate [Bi(NO₃)₃·5H₂O] were purchased from Aldrich Chemical Co. All chemicals were commercial materials of the highest available purity, and they were used as received. Commercial methyl violet 2B (MV2B) dye was provided by Roshfrans company, and it was employed as received.

Preparation of ZnCrBi-LDH

The ZnCrBi-LDH with molar ratio of 2.0:0.7:0.3 was prepared by a simple co-precipitation method. In a typical procedure, 1.0 g (3.36 mmol) of Zn(NO₃)₂·6H₂O and 0.47 g (1.18 mmol) of Cr(NO₃)₃·9H₂O were dissolved in 30 mL of deionized water to form a clear mixed salt solution (Solution A). 0.25 g (0.50 mmol) of Bi(NO₃)₃·5H₂O was dissolved in concentrated nitric acid solution (Solution B). Then, the above two saline solutions and a mixture containing NaOH (2 M) and Na₂CO₃ (0.5 M) were added simultaneously to a three-necked flask at a speed of 1 drop s⁻¹. The pH of resulting suspension was maintained at 9–10 by continuous addition of a 1 M NaOH and the mixed solution stirring for 12 h, and then, it was sonicated for 1 h. Finally, the mixture was transferred to Teflon-lined stainless steel autoclaves and the hydrothermal temperature is 160 °C for another 24 h. The resulting solid product was separated by centrifugation, washed with deionized water several times until pH 7, and dried in an oven at 80 °C for 6 h to collect the solid powder ZnCrBi-LDH. Also, ZnCr-LDH with 2.0:1.0 molar ratios was prepared by similar procedure without using Bi.

Photocatalytic experiments

Photocatalytic activities of all the samples were evaluated by degradation of the aqueous methylene blue (MB; molecular weight, 319.85 g/mol) as model pollutant under visible light irradiation. MB is a cationic dye, used extensively for dyeing cotton, wool, and silk. The risks of the existence of this dye in wastewater have arisen from the burns effect of eye, nausea, vomiting, and diarrhea. MB has a maximum absorption in the 660 nm visible area. MB is chosen as a model contaminant to evaluate the photocatalytic activity of prepared samples due to its stability under visible light irradiation. Chemical structure of methylene blue (C₁₆H₁₈N₃SCl) makes it to fall under a group of azin dyes, as shown in Scheme 1. The photocatalytic reaction was carried in a 50-mL single-compartment cylindrical quartz reactor containing 2 ppm of MB aqueous solution



Scheme 1 Structure of methylene blue (MB)

and 20 mg as-prepared photocatalysts. The solution was vigorously stirred with a magnetic stirrer. A 200-W xenon lamp was used as a light source with a UV filter to provide visible light. The luminous intensity of the xenon lamp was 100 mW/cm^2 . The actual experiments were performed at room temperature. Prior to illumination, the solution containing MB and photocatalyst magnetically was stirred for 120 min in the dark to ensure the establishment of an adsorption–desorption equilibrium between the photocatalyst and MB. Then, the solution was exposed to visible light irradiation under magnetic stirring for 120 min. At certain time intervals, specific amount of the solution was withdrawn and the changes in concentration of MB were observed using a UV–Vis spectrophotometer.

Characterization techniques

FTIR spectra were recorded on Jasco-680 (Japan) spectrophotometer with 4 cm^{-1} resolution. The KBr pellet technique was applied for monitoring changes in the FTIR spectra of the samples in the range of $4000\text{--}400 \text{ cm}^{-1}$. The vibrational transition frequencies are reported in wave numbers (cm^{-1}). XRD (Philips X' Pert Pro MPD) studies were performed to identify the formation of crystal phase by using Cu $K\alpha$ radiation ($\lambda = 0.1542 \text{ nm}$). The diffraction patterns were collected between 2θ of 5° and 80° at a scanning rate of $0.05^\circ/\text{min}$. The morphology of the samples was examined by FESEM (HITACHI; S-4160). The powdered sample was dispersed in H_2O , and then, the sediment was dried at room temperature before gold coating. Transmission electron microscopy (TEM) images of the samples were collected on a Philips CM120 transmission electron microscope with accelerator voltage of 100 kV. The UV–Vis absorption spectra were recorded using UV–Vis–NIR spectrophotometer with an integrating sphere (DUV-3700, Shimadzu, Japan), in which BaSO_4 was used as a reference.

Results and discussion

FTIR study

FTIR spectra of ZnCr-LDH and ZnCrBi-LDH are shown in Fig. 1. In these spectra, the broad absorption band in

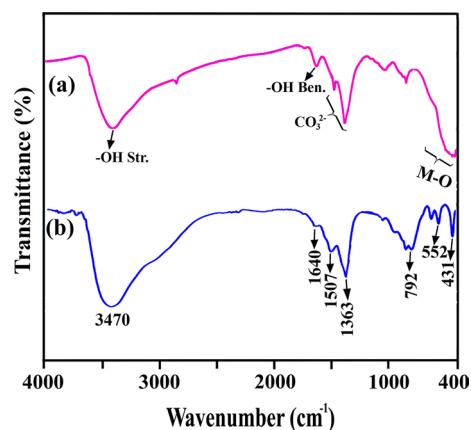


Fig. 1 FTIR spectra of the **a** ZnCr-LDH and **b** ZnCrBi-LDH

the region $3100\text{--}3600 \text{ cm}^{-1}$ is assigned to the OH stretching vibrations, $\nu(\text{OH})$, associated with the basal hydroxyl groups and interlayer water. The characteristic band of angular deformation in water molecules, $\delta(\text{H-O-H})$, is observed at 1640 cm^{-1} . The O–C–O asymmetric stretching vibration appears between 1363 and 1507 cm^{-1} . Compared with CO_3^{2-} of CaCO_3 (1430 cm^{-1}), there is a considerable lower shifted absorption peak at 1365 cm^{-1} , which shows that there was an intercalation between CO_3^{2-} and interlayer H_2O through the strong hydrogen bonding. The bands at lower wavenumbers such as 792 , 552 , and 431 cm^{-1} can be assigned to the metal–oxygen stretching modes (Zn–O, Cr–O, and Bi–O). These results confirmed the formation of LDHs (Fig. 1).

X-ray diffraction

XRD is one of the most useful techniques to analyze the layered structure of nanomaterials. The XRD patterns of ZnCr-LDH and ZnCrBi-LDH samples with ZnCrBi mole ratios of 2.0:0.7:0.3 are shown in Fig. 2. As shown in Fig. 2a, it can be seen that ZnCr-LDH has strong peaks at $2\theta = 11.6^\circ$, 23.7° , 34.6° , 39.7° , 46.3° , 61.56° , and 63.8° corresponding to (0 0 3), (0 0 6), (0 0 9), (0 1 5), (0 1 8), (110), and (1 1 3) planes, respectively. It is clear that ZnCr-LDH has hexagonal structure reported in the literature (JCPDS No. 05-0669), which almost has no change with ZnCrBi-LDH in the diffraction peaks position (Fig. 2b). All of the samples exhibit the characteristic diffraction peak of layered hydroxide-like materials, indicating that the bismuth does not destroy layered structure of the LDH, whereas a gradual decline in the intensity of (0 0 3) reflection peak and a significant broadening of (0 0 9) reflection were observed in the patterns of ZnCrBi-LDH. The broadness of the peaks in Fig. 2b indicates the low crystallinity of the ZnCrBi-LDH.

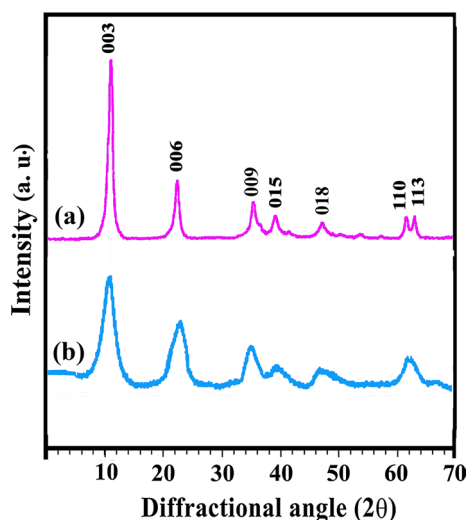


Fig. 2 XRD patterns of the **a** ZnCr-LDH and **b** ZnCrBi-LDH

FESEM and EDX study

The surface morphologies and microstructural details of the as-synthesized photocatalysts were examined by SEM, EDS, and TEM measurements. Figure 3 shows the FESEM images as well as the EDS pattern of the ZnCr-LDH. The ZnCr-LDH showed the nature of LDH particles which roughly consists of plate-like shape stacked on top of each other with lateral dimensions ranging over few micrometer and thickness over few hundred nanometers. Additionally, EDX pattern of the ZnCr-LDH indicates the elements of Zn and Cr and confirmed the formation of the LDH. The

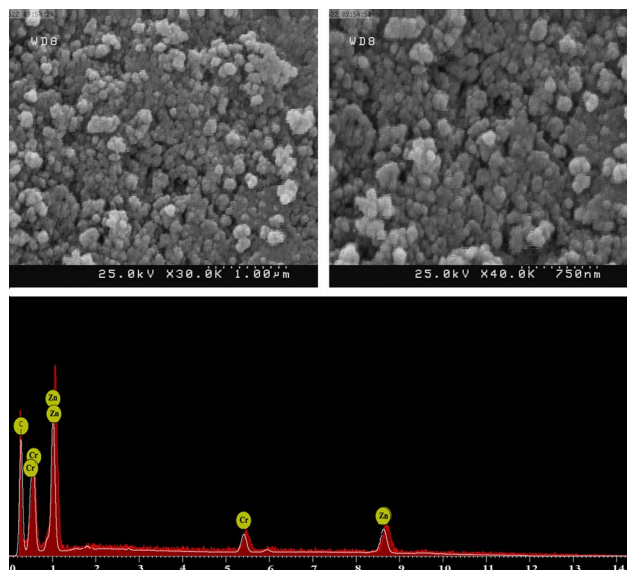


Fig. 3 FESEM photographs and EDS pattern of the ZnCr-LDH sample

morphological feature of the Bi-doped ZnCr-LDH (ZnCrBi-LDH) has globular shape compared to the ZnCr-LDH which has plate-like shape (Fig. 4). The presence of Bi in the LDH was also confirmed by EDX techniques as shown in Fig. 4.

TEM study

TEM picture presented an actual image of nanoclay platelets to permit recognition of internal morphology of nano-hybrids. TEM image of ZnCr-LDH and ZnCrBi-LDH samples as illustrated in Fig. 5a–d showed that the synthesized LDH is smooth overlapping crystals, and they are approximately in hexagonal form. As can be seen, the LDH sheets have homogeneous contrast, reflecting their ultrathin nature and uniform thickness. These were commonly observed for typical LDH compounds. The ZnCr-LDH and ZnCrBi-LDH samples have particle size around 20–40 nm.

Optical measurements

The light absorbance of the ZnCr-LDH and ZnCrBi-LDH samples was evaluated by the UV–Vis diffuse reflection absorption spectra, and the results are shown in Fig. 6. As shown in Fig. 6, the ZnCrBi-LDH exhibits enhanced absorption in visible light region (centered at 586 nm) in comparison with ZnCr-LDH (centered at 394 nm). The strong absorption band in the region of 394 nm which can be assigned to typical in Zn(II) coordinated to the CO_3^{2-} gallery [31–33]. Meanwhile, a broad absorption band from ~400 to 700 nm which is observed with maxima at ~586 nm may indicate the presence of Bi^{3+} or d–d

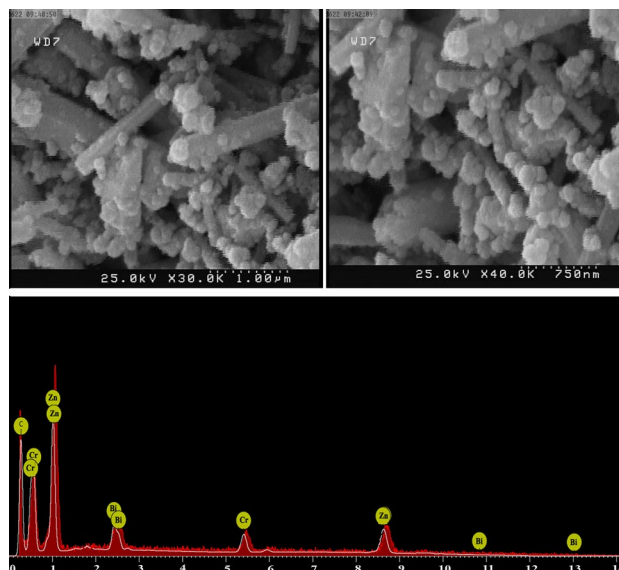


Fig. 4 FESEM photographs and EDS pattern of the ZnCrBi-LDH sample

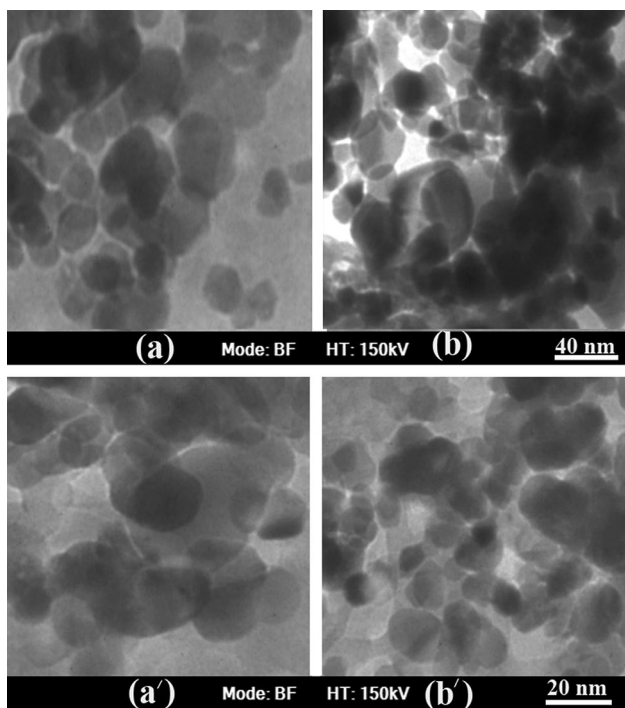


Fig. 5 TEM micrographs of the **a, a'** ZnCr-LDH and **b, b'** ZnCrBi-LDH

transition of Cr³⁺ in the brucite-like sheets [34–36]. The broad nature of absorption at ~586 nm could be ascribed to supramolecular guest–guest (hydrogen bonding and van der Waals forces) or guest–host interactions (electrostatic attraction, hydrogen bonding and van der Waals forces) [31–33]. In case of the layered materials, the UV spectrum shows an overall broadening and a red shift is observed due to higher aggregate formation.

Photocatalytic activity of ZnCr-LDH and ZnCrBi-LDH samples

Photocatalytic activity of different samples was followed through degradation of methylene blue as a function of irradiation time with visible light. To get the response of photocatalytic activities of ZnCr-LDH and ZnCrBi-LDH samples, the absorption spectra of exposed samples at various time intervals were recorded and the rate of color degradation was observed in terms of change in intensity at λ_{max} of the dye. The photodegradation yield is defined as:

$$\text{Photo degradation yield (\%)} = [(C_0 - C)/C_0] \times 100 \quad (1)$$

where C₀ and C are the initial concentration and concentration of dyes after photodegradation under visible light irradiation at various time intervals, respectively. In order to obtain the real photodegradation yield, the decreases in the dye concentration because of the adsorption and direct

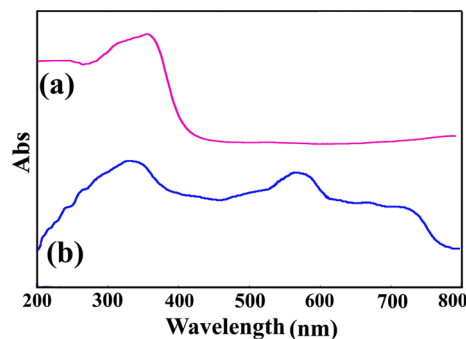


Fig. 6 UV–Vis spectra of the **a** ZnCr-LDH and **b** ZnCrBi-LDH

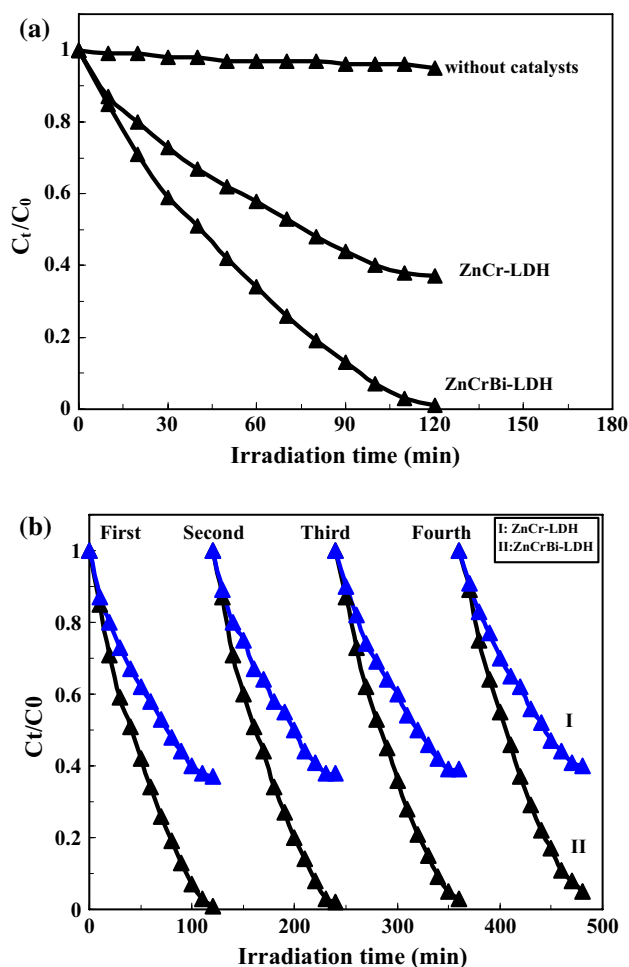


Fig. 7 **a** Photocatalytic degradation of MO over the different samples under visible light irradiation. **b** Photocatalyst stability test of prepared sample

photolysis should be deducted. The photocatalysis of MB is negligible without the presence of ZnCr-LDH and ZnCrBi-LDH samples, suggesting that the degradation of RhB is induced by photocatalysis. Figure 7a shows the photodegradation rate of MB under visible light in the presence

of different samples. MB can be completely decomposed within 120 min by the ZnCrBi-LDH heterojunction under visible light irradiation, which needs much less time than that of the ZnCr-LDH sample. After exposing the samples and MB dye under visible light for 120 min, the MB concentrations decreased dramatically with the ZnCrBi-LDH and ZnCr-LDH composite, i.e., about 99 and 63% of the MB dye was degraded by the ZnCrBi-LDH and ZnCr-LDH composite, respectively. The higher photocatalytic activity of ZnCrBi-LDH sample can be attributed to the combined effect of various factors: the bismuth doping, the effect of surface morphology on the surface area of these samples, and the increased light-harvesting ability (capability to absorb visible light and higher light absorption, compared to ZnCr-LDH). The kinetics of the decolorization of organic dyes has often been modeled with the following Langmuir–Hinshelwood equation [37, 38]:

$$\ln(C_0/C) = k_{\text{app}}t \quad (2)$$

where k_{app} is the apparent pseudo-first-order reaction rate constant and t is the reaction time. So degradation kinetics of methylene blue was studied by plotting the natural logarithm of concentration ratio $\ln(C/C_0)$ versus the irradiation time. The degradation process follows pseudo-first-order kinetics, and the degradation rate constant calculated from the slope of the kinetics plot was found to be 0.0084 and 0.0333 min^{-1} for ZnCr-LDH and ZnCrBi-LDH samples, respectively. Regeneration of catalyst is one of the key aspects to make heterogeneous catalysis technology for practical applications. The stability and reusability of the ZnCr-LDH and ZnCrBi-LDH catalysts were carried out with the same ratio of catalyst and dye concentration. After each reaction run, the catalyst was separated from the reaction system and its reusability was also investigated carefully. The catalyst was washed several times with distilled water, dried, and reused. Each cycle was carried out in the dark for 120 min and then exposed under visible light for 120 min. As shown in Fig. 7b, after a four-cycle experiment, these catalysts exhibited similar catalytic performance without significant deactivation. The above results revealed that these composites are potential catalysts with good photocatalytic activity, stability, and reusability.

Conclusions

In summary, ZnCr-LDH and ZnCrBi-LDH composites were synthesized by co-precipitation method. The characteristics of the obtained samples were investigated by SEM, TEM, XRD, FTIR, EDX, and UV–Vis. Photocatalytic experiments showed that ZnCrBi-LDH catalyst displayed high photocatalytic activity as compared to ZnCr-LDH under xenon light irradiation because of the increased

surface area and light-harvesting ability. Kinetic research showed that the reaction rate constant of ZnCrBi-LDH sample is approximately 1.4 times higher than the reaction rate constant of ZnCr-LDH. The stability of the samples indicated no observable performance degradation for prepared photocatalyst even after four recycles. Therefore, these prepared composites would have a widely applied prospect in photocatalytic field to eliminate the organic pollutants from wastewater.

Acknowledgements The authors are grateful to the Research Affairs Division Isfahan University of Technology (IUT), Isfahan, for partial financial support. Additional financial support from National Elite Foundation (NEF) and Iran Nanotechnology Initiative Council (INIC) is gratefully acknowledged.

Compliance with ethical standards

Conflict of interest The authors declare that they have no conflict of interest.

References

1. W. Wu, C. Jiange, V.A.L. Roy, Recent progress in magnetic iron oxide-semiconductor composite nanomaterials as promising photocatalysts. *Nanoscale* **7**, 38–58 (2015)
2. X.B. Chen, S.S. Mao, Titanium dioxide nanomaterials: synthesis, properties, modifications, and applications. *Chem. Rev.* **107**, 2891–2959 (2007)
3. T. Yan, W. Guan, W. Li, J. You, Ag_3PO_4 photocatalysts loaded on uniform SiO_2 supports for efficient degradation of methyl orange under visible light irradiation. *RSC Adv.* **4**, 37095–37099 (2014)
4. D.K. Zhong, D.R. Gamelin, Photoelectrochemical water oxidation by cobalt catalyst (“Co–Pi”)/ $\alpha\text{-Fe}_2\text{O}_3$ composite photoanodes: oxygen evolution and resolution of a kinetic bottleneck. *J. Am. Chem. Soc.* **132**, 4202–4207 (2010)
5. S. Baruah, M.N. Khan, J. Dutta, Perspectives and applications of nanotechnology in water treatment. *Environ. Chem. Lett.* **14**, 1–14 (2016)
6. H. Zhang, H. Ming, S. Lian, H. Huang, H. Li, L. Zhang, Y. Liu, Z. Kang, S.T. Lee, Fe_2O_3 /carbon quantum dots complex photocatalysts and their enhanced photocatalytic activity under visible light. *Dalton Trans.* **40**, 10822–10825 (2011)
7. R. Miao, Z. Luo, W. Zhong, Y. Zhang, S.L. Suib, Mesoporous TiO_2 modified with carbon quantum dots as a high-performance visible light photocatalyst. *Appl. Catal. B Environ.* **189**, 26–38 (2016)
8. X.L. Fang, C. Chen, M.S. Jin, Q. Kuang, Z.X. Xie, S.Y. Xie, R.B. Huang, L.S. Zheng, Single-crystal-like hematite colloidal nanocrystal clusters: synthesis and applications in gas sensors, photocatalysis and water treatment. *J. Mater. Chem.* **19**, 6154–6160 (2009)
9. D. Chatterjee, S. Dasgupta, Visible light induced photocatalytic degradation of organic pollutants. *J. Photochem. Photobiol., C* **6**, 186–205 (2005)
10. M. Matsuoka, M. Kitano, M. Takeuchi, M. Anpo, J.M. Thomas, Photocatalysis for new energy production. Recent advances in photocatalytic water splitting reactions for hydrogen production. *Catal. Today* **122**, 51–61 (2007)
11. P. Tang, H. Chen, F. Cao, G. Pan, Magnetically recoverable and visible-light-driven nanocrystalline YFeO_3 photocatalysts. *Catal. Sci. Technol.* **1**, 1145–1148 (2011)

12. J. Ma, J. Ding, L. Yu, L. Li, Y. Kong, S. Komarneni, BiOCl dispersed on NiFe-LDH leads to enhanced photo-degradation of Rhodamine B dye. *Appl. Clay Sci.* **109–110**, 76–82 (2015)
13. J.C. Hu, Z. Song, L.F. Chen, H.J. Yang, J.L. Li, R. Richards, Adsorption properties of MgO(111) nanoplates for the dye pollutants from wastewater. *J. Chem. Eng. Data* **55**, 3742–3748 (2010)
14. M.M.F. Silva, M.M. Oliveira, M.C. Avelino, M.G. Fonseca, R.K.S. Almeida, E.C. Silva Filho, Adsorption of an industrial anionic dye by modified-KSF montmorillonite: evaluation of the kinetic, thermodynamic and equilibrium data. *Chem. Eng. J.* **203**, 259–268 (2012)
15. M. Dinari, G. Mohammadnezhad, R. Soltani, Fabrication of poly(methyl methacrylate)/silica KIT-6 nanocomposites via in situ polymerization approach and their application for removal of Cu^{2+} from aqueous solution. *RSC Adv.* **6**, 11419–11429 (2016)
16. Q. Zhou, F. Chen, W. Wu, R. Bu, W. Li, F. Yang, Reactive orange 5 removal from aqueous solution using hydroxyl ammonium ionic liquids/layered double hydroxides intercalation composites. *Chem. Eng. J.* **285**, 198–206 (2016)
17. L. Mohapatra, K.M. Parida, Zn–Cr layered double hydroxide: visible light responsive photocatalyst for photocatalytic degradation of organic pollutants. *Sep. Purif. Technol.* **91**, 73–80 (2012)
18. L. Mohapatra, K.M. Parida, Recent progress in the development of carbonate-intercalated Zn/Cr LDH as a novel photocatalyst for hydrogen evolution aimed at the utilization of solar light. *Dalton Trans.* **41**, 1173–1178 (2012)
19. L. Mohapatra, K.M. Parida, Dramatic activities of vanadate intercalated bismuth doped LDH for solar light photocatalysis. *Phys. Chem. Chem. Phys.* **16**, 16985–16996 (2014)
20. Y.F. Sun, S. Gao, Y. Xie, Atomically-thick two-dimensional crystals: electronic structure regulation and energy device construction. *Chem. Soc. Rev.* **43**, 530 (2014)
21. B. Benalioua, M. Mansour, A. Bentouami, B. Boury, E.H. Elandaloussi, The layered double hydroxide route to Bi–Zn co-doped TiO_2 with high photocatalytic activity under visible light. *J. Hazard. Mater.* **288**, 158–167 (2015)
22. A.A. Ensafi, M. Jafari-Asl, A. Nabiyani, B. Rezaei, M. Dinari, Hydrogen storage in hybrid of layered double hydroxides/reduced graphene oxide using spillover mechanism. *Energy* **99**, 103–114 (2016)
23. M. Dinari, M.M. Momeni, Y. Ghayeb, Photodegradation of organic dye by ZnCrLa-layered double hydroxide as visible-light photocatalysts. *J. Mater. Sci. Mater. Electron.* **27**, 9861–9869 (2016)
24. M.A. Oliver-Tolentino, J. Vázquez-Samperio, A. Manzo-Robledo, R.G. González-Huerta, J.L. Flores-Moreno, D. Ramírez-Rosales, A. Guzmán-Vargas, An approach to understanding the electrocatalytic activity enhancement by super exchange interaction toward OER in alkaline media of Ni–Fe LDH. *J. Phys. Chem. C* **118**, 22432–22438 (2014)
25. M. Dinari, P. Asadi, S. Khajeh, In situ thermal synthesis of novel polyimide nanocomposite films containing organo-modified layered double hydroxide: morphological, thermal and mechanical properties. *New J. Chem.* **39**, 8195–8203 (2015)
26. L. Yao, D. Wei, D. Yan, C. Hu, ZnCr layered double hydroxide (LDH) nanosheets assisted formation of hierarchical flower-like CdZnS@LDH microstructures with improved visible-light-driven H_2 production. *Chem. Asian J.* **10**, 630–636 (2015)
27. A. Guzmán-Vargas, E. Lima, G.A. Uriostegui-Ortega, M.A. Oliver-Tolentino, E.E. Rodríguez, Adsorption and subsequent partial photodegradation of methyl violet 2B on Cu/Al layered double hydroxides. *Appl. Surf. Sci.* **363**, 372–380 (2016)
28. S. Mallakpour, M. Dinari, Effect of organically modified Ni–Al layered double hydroxide loading on the thermal and morphological properties of L-methionine containing poly(amide-imide) nanocomposites. *RSC Adv.* **5**, 28007–28013 (2015)
29. P. Roy Chowdhury, K.G. Bhattacharyya, Synthesis and characterization of Co/Ti layered double hydroxide and its application as a photocatalyst for degradation of aqueous Congo Red. *RSC Adv.* **5**, 92189–92206 (2015)
30. Y. Zhao, X. Jia, G.I.N. Waterhouse, L.-Z. Wu, C.-H. Tung, D. O’Hare, T. Zhang, Layered double hydroxide nanostructured photocatalysts for renewable energy production. *Adv. Energy Mater.* **1501974**, 1–20 (2015)
31. K.M. Parida, L. Mohapatra, Carbonate intercalated Zn/Fe layered double hydroxide: a novel photocatalyst for the enhanced photo degradation of azo dyes. *Chem. Eng. J.* **179**, 131–139 (2012)
32. P.R. Chowdhury, K.G. Bhattacharyya, Ni/Ti layered double hydroxide: synthesis, characterization and application as a photocatalyst for visible light degradation of aqueous methylene blue. *Dalton Trans.* **44**, 6809–6824 (2015)
33. M.M. Khan, S.A. Ansari, D. Pradhan, M.O. Ansari, D.H. Hang, J. Lee, M.H. Cho, Band gap engineered TiO_2 nanoparticles for visible light induced photoelectrochemical and photocatalytic studies. *J. Mater. Chem. A* **2**, 637–644 (2014)
34. K. Parida, L. Mohapatra, N. Baliarsingh, Effect of Co^{2+} Substitution in the framework of carbonate intercalated Cu/Cr LDH on structural, electronic, optical, and photocatalytic properties. *J. Phys. Chem. C* **116**, 22417–22424 (2012)
35. W. He, R. Wang, L. Zhang, J. Zhu, X. Xiang, F. Li, Enhanced photoelectrochemical water oxidation on a BiVO_4 photoanode modified with multi-functional layered double hydroxide nanowalls. *J. Mater. Chem. A* **3**, 17977–17982 (2015)
36. L. Mohapatra, K.M. Parida, A review on recent progress, challenges and perspective of layered double hydroxides as promising photocatalysts. *J. Mater. Chem. A* **4**, 10744–10766 (2016)
37. M.M. Momeni, Y. Ghayeb, Photochemical deposition of platinum on titanium dioxide-tungsten trioxide nanocomposites: an efficient photocatalyst under visible light irradiation. *J. Mater. Sci. Mater. Electron.* **27**, 1062–1069 (2016)
38. M.M. Momeni, Y. Ghayeb, Fabrication and characterization of zinc oxide-decorated titania nanoporous by electrochemical anodizing-chemical bath deposition techniques: visible light active photocatalysts with good stability. *J. Iran Chem. Soc.* **1**, 481–488 (2016)